JACS
JOURNAL OF THE AMERICAN CHEMICAL SOCIETY

ARTICLE

pubs.acs.org/JACS

# Organization of Bacteriochlorophylls in Individual Chlorosomes from *Chlorobaculum tepidum* Studied by 2-Dimensional Polarization Fluorescence Microscopy[#]

Yuxi Tian,[†] Rafael Camacho,[†] Daniel Thomsson,[†] Michael Reus,[‡] Alfred R. Holzwarth,[*,‡] and Ivan G. Scheblykin[*,†]

[†]Chemical Physics, Lund University, Box 124, 22100, Lund, Sweden

[‡]Max-Planck-Institut für Bioanorganische Chemie, D-45470 Mülheim an der Ruhr, Stiftstr. 34-36, Germany

Supporting Information

**ABSTRACT:** Chlorosomes are the largest and most efficient natural light-harvesting systems and contain supramolecular assemblies of bacteriochlorophylls that are organized without proteins. Despite a recent structure determination for chlorosomes from *Chlorobaculum tepidum* (Ganapathy et al. Proc. Natl. Acad. Sci. U.S.A. 2009, 106, 8525), the issue of a possible large structural disorder is still discussed controversially. We have studied individual chlorosomes prepared under very carefully controlled growth condition by a novel 2-dimensional polarization single molecule imaging technique giving polarization information for both fluorescence excitation and emission simultaneously. Contrary to the existing literature data, the polarization degree or modulation depth ($M$) for both excitation (absorption) and emission (fluorescence) showed extremely narrow distributions. The fluorescence was always highly polarized with $M \approx 0.77$, independent of the excitation wavelength. Moreover, the fluorescence spectra of individual chlorosomes were identical within the error limits. These results lead us to conclude that all chlorosomes possess the same type of internal organization in terms of the arrangement of the bacteriochlorophyll c transition dipole moments and their total excitonic transition dipole possess a cylindrical symmetry in agreement with the previously suggested concentric multitubular chlorophyll aggregate organization (Ganapathy et al. Proc. Natl. Acad. Sci. U.S.A. 2009, 106, 8525).

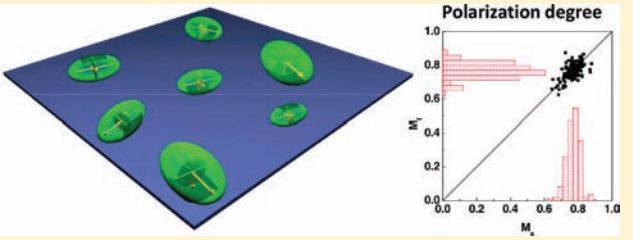


## INTRODUCTION

Chlorosomes, the natural light-harvesting systems of green bacteria, are the largest and most efficient antenna systems that exist in nature.[1] They have recently become the role models for the design of supramolecular artificial light-harvesting systems.[2−4] A chlorosome contains hundreds of thousands of bacteriochlorophyll (BChl) c, d, or e molecules, which are self-organized in a supramolecular arrangement without the interaction with proteins[5,6] (see refs 7 and 8 for recent reviews). The BChl building blocks form strongly excitonically coupled systems as in J-type aggregates.[9,10] The excitonic coupling gives rise to a strongly red-shifted absorption spectrum and an extremely large exciton diffusion length.[11] For a long time it had not been possible to experimentally obtain a molecular structure of the BChl organization. Since chlorosomes come in different sizes, crystallization is not possible and detailed structural characterization had to resort to other methods. Thus many studies have been devoted to reveal structure information using a variety of optical spectroscopies[12−18] combined with molecular modeling.[19] In particular solid-state NMR methods have been employed for determining the short-range organization of the BChls, that is, intermolecular carbon−carbon distances on a scale less than 5 Å.[20−22] X-ray scattering and high resolution electron microscopy were employed as well for determining the long-range order on a scale above 10 Å[22−27] (see refs 1, 7, 8, and 28 for recent review articles). The most advanced structure determination, seeking to combine all information on the short-range as well as the long-range organization into a single structure, used a combination of solid-state NMR methods and high-resolution cryo-EM. The combined analysis resulted in a concentric multitubular arrangement of the BChl aggregates in a pigment mutant of *Chlorobaculum tepidum* chlorosomes[22,27] (Figure 1a). In contrast to the mutant, the wild type (w.t.) structure was structurally less well-resolved however and displayed some long-range disorder,[22,27] although the overall structure, in particular the short-range arrangement of BChls, was also found to be the same as in the mutant. Taken together the information for both long-range and short-range also resulted in a multitubular arrangement. While a part of the disorder found in the w.t. chlorosomes is certainly because of the mixture of different BChl c isomers, the major reason for the disorder observed in the EM pictures is not well understood and is still a matter of debate with several alternative models under discussion[22,25] (c.f. Figure 1). The undulated lamellar structure (Figure 1b) has been

**Received:** March 4, 2011
**Published:** September 16, 2011

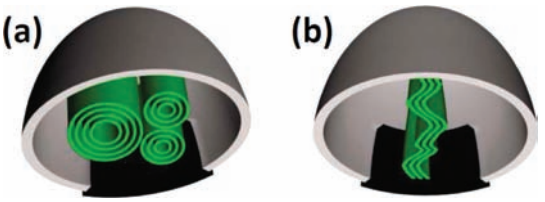


**Figure 1.** Alternative models for the long-range BChl organization in chlorosomes: (a) concentric multicylindrical structure,[22,27] (b) undulated lamellar structure;[23] only three undulated lamellar sheets are shown for clarity, for full details see ref 23.

proposed based on cryo-electron microscopy and X-ray diffraction for w.t. chlorosomes of *C. tepidum*.[23] It should be pointed out however that the latter structure has been shown to be inconsistent with recent more detailed cryo-electron microscopy and solid state NMR data.[22,27] Another point worth considering is that the detailed structure might depend to some extent on the growth conditions.[29]

Polarization spectroscopy is a powerful method to determine structural information of pigment arrangements by following the transition dipole moment orientations in complex molecular systems. It should thus be able, in particular if combined with single molecule techniques, to give valuable information about the internal organization of the BChls in chlorosomes and hopefully to distinguish between the different proposed models. The relative orientation of transition dipoles in chlorosomes was previously characterized by polarization spectroscopy.[17,30,31] Single molecule spectroscopy (SMS) has also been employed to investigate individual chlorosomes by studying their fluorescence spectra and anisotropy.[32−34] Despite these efforts, the results obtained by ensemble anisotropy studies as well as by SMS techniques so far are not sufficient to either confirm or challenge the proposed structural arrangements (c.f., Figure 1). In this work, a recently developed 2-dimensional (2D) polarization SMS technique[35] was used to study individual chlorosomes grown and isolated under very mild and carefully controlled conditions from w.t. *C. tepidum* bacteria. One of the main advantages of this technique is that the polarization degree (or modulation depth) of both absorption and fluorescence are obtained simultaneously for every individual chlorosome, and it can even provide additional information about energy transfer processes. The results unambiguously show uniformity of polarization properties of different chlorosomes and a cylindrical symmetry of the total transition dipole moment along the long axis of the chlorosome.

## EXPERIMENTAL SECTION

**Sample Preparation.** *C. tepidum* was grown anaerobically at 40 °C in a growth medium[36] in 1.5 L continuously stirred reactor bottles under illumination with fluorescent tubes (Osram, mixture of 18W/25 universal-white and 18W/77 Fluora) using illumination intensities of 25 $\mu$E/(s·m$^2$) for WTLL chlorosomes (chlorosomes from w.t. *C. tepidum* bacteria grown under low light condition) and 125 $\mu$E/(s·m$^2$) for WTHL chlorosomes (chlorosomes from w.t. *C. tepidum* bacteria grown under high light condition) at the surface of the bottles; 1.2 L of medium was inoculated with 75 mL freshly grown cell culture and grown for 1 day for light adaptation. Then, 75 mL of this light-adapted cell culture was inoculated as before with 1.2 L of fresh medium. Cells were harvested at the early logarithmic growth phase after 1 day of growth and chlorosomes were isolated as described in Gerola and Olson[37] with some

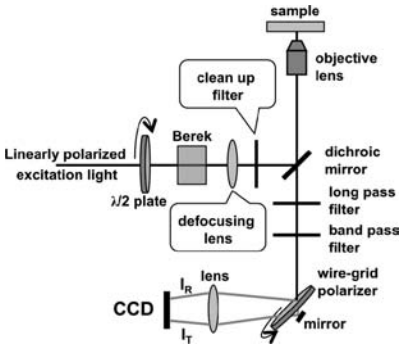


**Figure 2.** Illustration of the setup for 2D polarization fluorescence microscopy.

modifications. Cells were harvested by centrifugation at 12000 *g*. The pellet was resuspended in 20 mM Tris-HCl, pH 8.0, 2 M NaSCN, 10 mM sodium ascorbate. After French press treatment, the suspension was centrifuged at 21000 *g* for 20 min. The enriched chlorosome fraction was separated and layered on a linear 10−40% sucrose gradient in the same medium. Density gradient centrifugation was carried out for 16 h at 12500 *g*. The chlorosomes enriched in the 25% sucrose region of the gradient were collected. The sample, diluted 1:100 in buffer, was dialyzed using a 12K cutoff tube for 24 h against 20 mM Tris-HCl, pH 8.0 buffer. After dialysis, the chlorosome suspension in Tris buffer showed the expected VIS absorption maxima. This stock solution was kept in the dark around 4 °C until further use.

For single chlorosome studies the stock solution was diluted ∼50 times with 20 mM Tris-HCl buffer (pH 8.0). The diluted solution was then spin-cast on an untreated glass substrate (22 × 22 × 0.15 mm, Menzel, Germany) at 1400 rpm. The chlorosomes were thus attached to the glass surface, while the remaining thin water film evaporated rapidly. The sample was then transferred to a nitrogen atmosphere, which efficiently prevented photodegration during the measurements. At the concentration range used, a linear dependence between the number of bright spots per image and the concentration of chlorosome was observed (Figure S1, Supporting Information), which is an indication that we were working with single chlorosomes rather than with their aggregates. All spectroscopy and microscopy studies were carried out at room temperature.

**Single Chlorosome Spectroscopy.** For studying of individual chlorosomes, a home-built wide-field fluorescence microscope setup based on an Olympus IX-71 inverted microscope and Princeton instruments PhotonMAX 512 EMG CCD camera with on-chip multiplication gain was used.[38] The samples were excited at 458 nm (CW $Ar^+$ laser), at 633 nm by CW He−Ne laser or at 750 nm by CW Ti: Sapphire laser (Spectra-Physics, Model 3900S, CA). The fluorescence was collected by an oil immersion objective lens (Olympus, UPlanFLN, 60×, NA = 0.65, Japan) and imaged on the CCD camera. For the fluorescence spectra measurements, a transmission holographic diffraction grating (150 lines/mm, Thorlabs) was placed in front of the CCD camera. The spectral sensitivity was calibrated using a standard tungsten incandescent lamp and all spectra were corrected accordingly. The instrumental response function had a spectral full width at half-maximum (FWHM) of ∼6 nm.

**2D-Polarization Single Molecule Imaging.** 2-dimensional polarization imaging of individual chlorosomes was performed using the setup as shown in Figure 2 and described previously.[35,38] The sample is excited by linearly polarized light on the sample plane and the fluorescence passes through an analyzer before reaching the CCD camera. Assuming the fluorescence quantum yield is independent of the excitation polarization, the fluorescence intensity is directly proportional to the absorption of the excitation light. For the sake of simplicity,

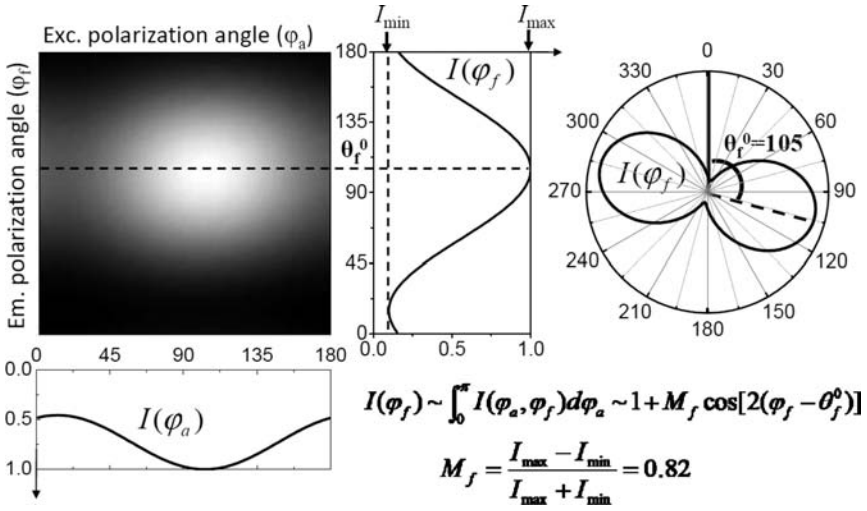


**Figure 3.** Experimental 2D polarization plot obtained for a randomly selected single chlorosome excited at 633 nm. This particular chlorosome had $M_f = 0.82$ and $M_a = 0.37$, the main emission transition of the chlorosome had an angle $\theta_f^0 = 105°$ with the *Y*-axis in the sample plane. The equation shows how to measure the modulation depth from the experimental 2D polarization plot.

we will subsequently use the term "polarization properties in absorption" rather than "polarization properties in fluorescence excitation". Both the polarization angle of the excitation light ($\varphi_a$, where "a" stands for absorption) and the analyzer orientation angle ($\varphi_f$, where "f" stands for fluorescence) are rotated simultaneously with different frequencies. The fluorescence intensity $I(\varphi_a, \varphi_f)$ is measured as a function of these two angles $\varphi_a$ and $\varphi_f$ (Figure 3). By integration of the fluorescence intensity $I(\varphi_a, \varphi_f)$ over one of the angles ($\varphi_a$ or $\varphi_f$) as shown in Figure 3, we can get the angular dependences $I(\varphi_f)$ or $I(\varphi_a)$. The fluorescence modulation depth ($M_f$) and the fluorescence phase were thus obtained by fitting $I(\varphi_f)$ using the equation with parameters $M_f$, $\varphi_f$, and $\theta_f^0$, as shown in Figure 3. Modulation depth in absorption ($M_a$) and the absorption phase ($\theta_a^0$) are obtained in the same way. The difference between $\theta_a^0$ and $\theta_f^0$ was defined as the phase shift. More detailed description is given in Supporting Information.

## RESULTS

**Fluorescence Spectra of Individual Chlorosomes.** Fluorescence spectra of 20 individual WTHL chlorosomes were measured using 458 and 633 nm excitations (Figure 4). No variations of the spectra from chlorosome to chlorosome and no excitation wavelength dependence were observed within the limits of experimental errors (±3 nm). This unequivocally indicates the absence of any heterogeneity in terms of the spectral properties of individual chlorosomes. The individual spectra were also nearly identical to the spectrum of the bulk chlorosome solution. A small shoulder observed in the solution ensemble spectrum at ~676 nm can be clearly assigned to the fluorescence of a minor amount of free BChl c molecules.

Overall the fluorescence from BChl a in the baseplate (usually situated around 810 nm[28]) was rather weak both for individual chlorosomes as well for the ensemble in solution. The fluorescence from the baseplate is known to be small or absent under oxygenic conditions.[39,40] No efforts have been made to exclude oxygen in our sample preparations but a nitrogen atmosphere was kept around the sample during the measurements.

**Polarization Properties of Individual Chlorosomes.** Figure 5 shows the polarization correlation plots and the histograms of absorption and fluorescence modulations depths of WTHL

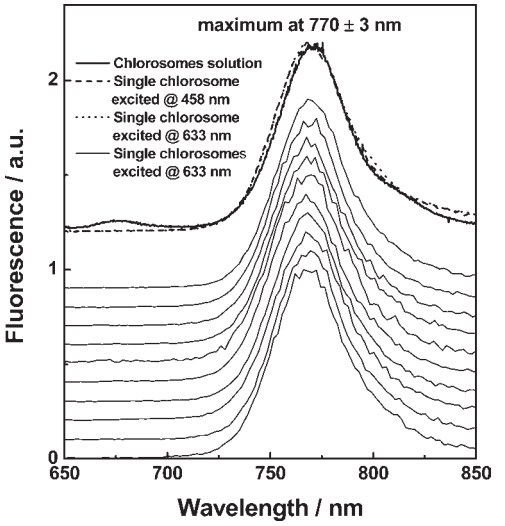


**Figure 4.** Fluorescence spectra of WTHL chlorosomes in bulk solution under 463 nm excitation (thick solid line) and for individual WTHL chlorosomes excited at 458 (dashed line) and 633 nm (dotted line). Spectra of 10 randomly selected individual chlorosomes excited at 633 nm are presented for comparison (thin solid lines).

chlorosomes when excited at 633, 458, and 750 nm. The data points are concentrated in small areas for all excitation wavelengths thus demonstrating very small differences between different chlorosomes regarding their polarization properties (Table 1). We attribute these differences to the experimental errors rather than physical differences between individual chlorosomes. The fluorescence modulation depth is almost the same (~0.77) for all excitation wavelengths while the absorption modulation depth is excitation wavelength dependent (Figure 5 and Table 1). Also the phase shifts for individual chlorosomes are very narrowly distributed around zero regardless of the excitation wavelength, indicating that $I(\varphi_a)$ and $I(\varphi_f)$ always have the same phase (Figure 6). The width of the distributions appears to be slightly different for different excitation wavelengths. This difference most likely reflects the limits of statistical and measurement accuracy.

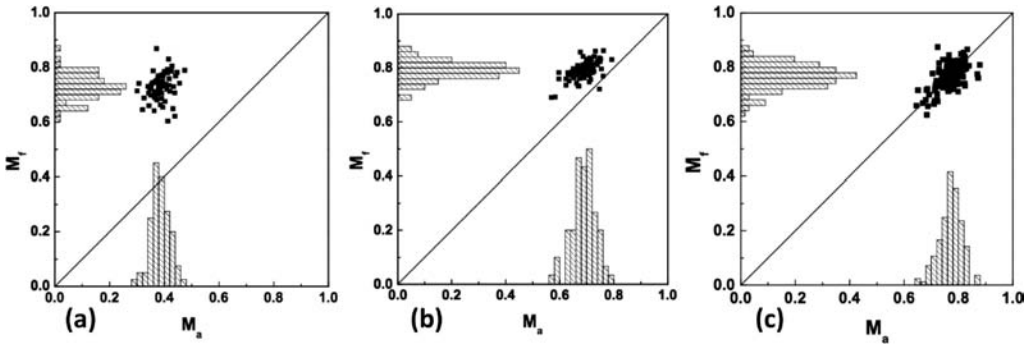


**Figure 5.** Histograms and correlation between the fluorescence ($M_f$) and absorption ($M_a$) modulation depths of WTHL chlorosomes excited at 633 (a), 458 (b), and 750 nm (c).

**Table 1. Absorption and Fluorescence Modulation Depths of WTHL Chlorosomes Obtained by Gaussian Fitting of the Distribution**

| exc. wavelength/nm | 458 | 633 | 750 |
|---|---|---|---|
| $M_a$ | 0.69 ± 0.04 | 0.38 ± 0.03 | 0.78 ± 0.04 |
| $M_f$ | 0.79 ± 0.03 | 0.73 ± 0.05 | 0.77 ± 0.04 |

## DISCUSSION

**Total Transition Dipole Moment.** The fluorescence spectral and polarization properties of single chlorosomes in our study appear to be very homogeneous. Basically, we could not see any difference between chlorosomes within error limits. This is different, for example, from previously reported large distributions in peak positions of the fluorescence of single chlorosomes.[41,42] The homogeneity of all the spectral properties of individual chlorosomes in our study suggests that our chlorosome preparation is much more homogeneous than previously reported ones. While our preparation method is not principally different from the traditional methods, we have taken great care providing homogeneity both in the growth conditions (i.e., homogeneous light intensity, low cell density, and short growth times) and in avoiding any harsh treatments during the isolation procedures (i.e., avoiding aggregation of chlorosomes by keeping concentration very low in all steps, by keeping the temperature constant, avoiding freezing/unfreezing cycles in the sample handling etc.). This preparation routine was also found to provide optimal resolution in electron microscopy.[22]

The total transition dipole moment of a chlorosomes has an excitonic origin and can be described by three mutually perpendicular components $\mu_1$, $\mu_2$, and $\mu_3$ (Scheme 1 block 1). The very narrow distribution and high values of the fluorescence modulation depths mean that all chlorosomes are essentially identical in their polarization properties. Note that if the BChls would be completely randomly oriented in 3D inside chlorosomes the modulation depth would also be narrowly distributed, in contrast to our experiments, around zero. However, because the modulation depths in our experiments are very high, the BChls must possess a distinct organization in terms of the orientation of their transition dipole moments. To fully interpret the polarization data we need to consider the orientation of the individual chlorosomes on the glass surface. The chlorosomes of *C. tepidum* are oblong bodies possessing large length/width/height ratios (100−200/40−100/10−30).[27] They orient well in stretched gels with their long axes parallel to the stretching axis. This property has been exploited to perform linear dichroism (LD)

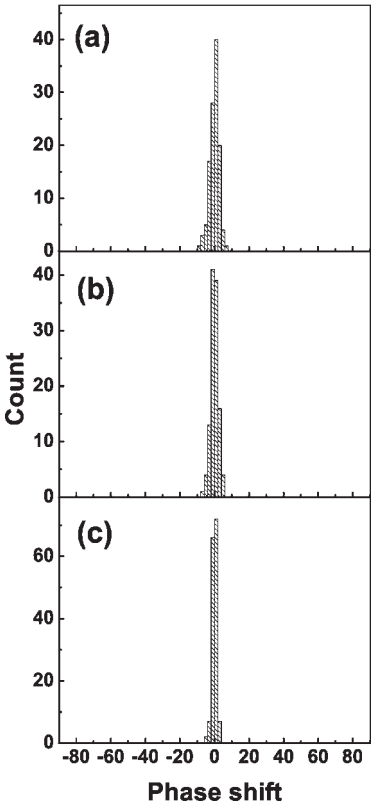


**Figure 6.** Histogram of the phase shift of the WTHL chlorosomes when excited at 633 (a), 458 (b), and 750 nm (c).

studies.[31,43] Because of their elongated shape, the chlorosomes in a spin-cast sample are laying on the surface with their long axis parallel to it, as seen by AFM experiments.[30] This does not however fully answer the question of how the chlorosomes are oriented in terms of rotation along the long axis, that is, whether there is a random or a preferred orientation of the baseplate to the glass surface. The envelopes of the chlorosomes are hydrophilic, formed by a single lipid layer except for the baseplate, which consists of CsmA proteins. Presumably the baseplate itself is less hydrophilic or even hydrophobic, since in the intact bacterial cytoplasmic membrane system it interacts with the FMO protein surrounded by an aqueous environment.[1] Based on the hydrophilicity argument, it is actually likely that chlorosomes should be able to orient more or less randomly around their long axis as long

**Scheme 1. Discussion Block Scheme about the Total Transition Dipole Moments of the Chlorosomes***

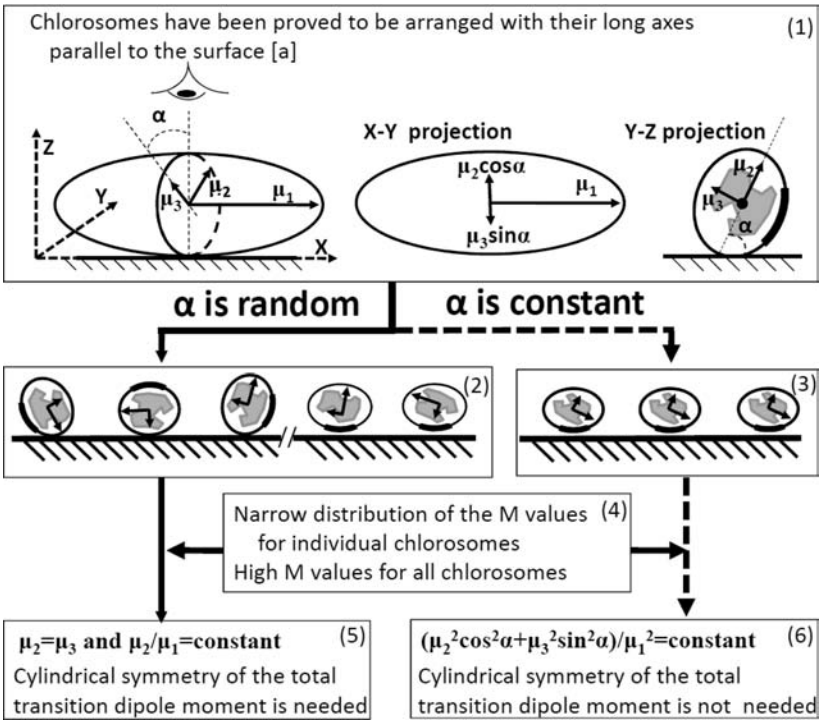


* $\mu_1, \mu_2$, and $\mu_3$ are the principal dipoles ($\mu_1 > \mu_2 > \mu_3$, as defined in ref 44.). The angle between $\mu_2$ and the surface is defined as $\alpha$. The dash arrows mean that this possibility has been excluded (see the text). [a] Proven by AFM and LD spectra.[28,30]

as the long axis remains parallel to the glass surface. In terms of the Scheme 1 it means that the angle $\alpha$ is more or less random. Then a cylindrical symmetry of the total transition dipole moment ($\mu_2 = \mu_3$) is necessary and also the ratio $\mu_2/\mu_1$ should be the same for different chlorosomes to have the homogeneity of the modulation depths observed experimentally (Scheme 1 block 4). However, we cannot entirely exclude a preferential interaction of the baseplate of the chlorosome with the glass surface. Even in this case, we still can have random $\alpha$ (meaning that the cylindrical symmetry is still necessary) if the orientation of the internal aggregate is not correlated strongly with the orientation of the base plate (Scheme 1 block 2). There exists a hypothetical situation that does not necessitate the cylindrical organizational symmetry of BChls when the values of the angle $\alpha$ are the same for all chlorosomes in the sample (for an example see Scheme 1 block 3) and the ratio $(\mu_2^2 \cos^2 \alpha + \mu_3^2 \sin^2 \alpha)/\mu_1^2$ is also the same for all chlorosome. Obviously such highly restrictive requirements make this situation very unlikely. Moreover, if we also consider that the high resolution EM data[22,27] did not show any preferential orientation of BChl aggregates relative to the baseplate this situation can be completely excluded. Thus we conclude the total transition dipole moment of a chlorosome possesses cylindrical symmetry along its long geometrical axis. Of course we cannot completely exclude a presence of asymmetrically organized pigments (e.g., flat lamellas); however, their contribution to the total light absorption and emission must be within the experimental errors of our measurements, see the discussion below.

At the first glance, it may appear that our conclusion is in contradiction with experiments of Shibata et al. who studied polarization properties of individual chlorosomes of *C. tepidum* at low temperature.[33] In contrast to our findings, the fluorescence

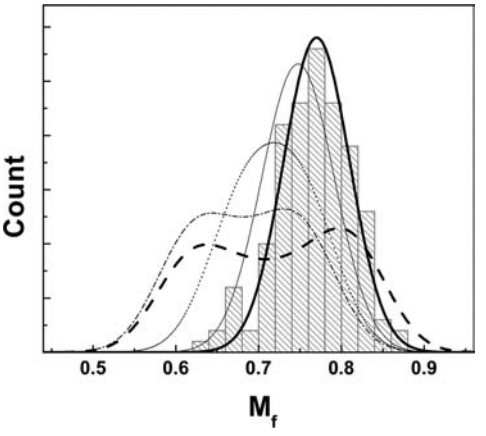


**Figure 7.** Comparison between the experimental modulation depth distribution obtained by us (gray bars) and the calculated ones obtained by using different models of the chlorosomes characterized by 3 principal dipoles as suggested in ref 33. Bold solid line: $\mu1/\mu2/\mu3$ = 1/0.36/0.36. Bold dash line: $\mu_1/\mu_2/\mu_3$ = 1/0.5/0.3 as suggested by Shibata et al.[33] Thin solid line: $\mu1/\mu2/\mu3$=1/0.36/0.40. Thin dotted line: $\mu1/\mu2/\mu3$ = 1/0.36/0.45. Thin dot dash line: $\mu1/\mu2/\mu3$=1/0.36/0.50. A Gaussian distribution was used assuming an experimental error of 0.04 for all the calculated models. The chlorosomes were allowed to have random orientations in terms of rotation along the long axis (see the situation in block 2 in the Scheme 1).

modulation depth in their work was widely distributed ranging from 0 to 0.8. Both random 3D orientation of the individual chlorosomes in the frozen medium, as well as absence of cylindrical symmetry of the transition dipole moments were proposed as reasons for the wide distribution of the observed

modulation depths of individual chlorosomes.[33] We tried to use the ratios of the principal dipole moments $\mu_1/\mu_2/\mu_3 = 1/0.5/0.3$ suggested by Shibata et al. to calculate the modulation depth distribution of the chlorosomes having random orientation along their long axis laying on the glass surface (Scheme 1 block 2). One can clearly see that the model distribution is incompatible with our experimental result (Figure 7). The experimental modulation depth distribution obtained in our experiment can be well fitted assuming the principal dipole moment ratios $\mu_1/\mu_2/\mu_3 = 1/(0.36 \pm 0.04)/(0.36 \pm 0.04)$ with a Gaussian distribution of the experimental error. The origin of the error lies in the limited signal-to-noise ratio and depolarization effects in the optics, which is difficult to compensate completely. To show how sensitive the distribution is to the breaking of the cylindrical symmetry of the transition dipole moment, we have added to the plot several distributions calculated for different degrees of asymmetry ($\mu_2 \neq \mu_3$) (Figure 7). This illustrates that the distributions are highly sensitive to any asymmetry. We thus conclude that the better controlled growth conditions and the avoidance of extremes in the isolation procedures resulted in an isolation of chlorosomes that is highly homogeneous in comparison to previously reported preparations. This implies however that native chlorosomes in intact green bacteria do possess a BChl organization that is much more homogeneous and regular than what was supposed so far based on the single chlorosome data and also the recent electron microscopy data.[22,27] The difference in the temperature (we measured at room temperature, whereas the data of Shibata et al. were obtained at 13 K) can have some effect too. In principle, some inhomogeneity observable at 13 K could be masked at room temperature due to energy level broadening and thermal population of higher energy states of the exciton band.

It is clear that the quite different measuring conditions of Shibata et al. resulted in a 3D distribution of the chlorosome orientation. Thus, before resorting to any conclusions about the degree of disorder and possible deviations of cylindrical pigment symmetry the effects of a nonrandom 3D orientation of the chlorosomes in the experiments of Shibata et al. would have to be taken into account in a quantitative model. It is quite possible however that the isolation procedures used in that work might have also resulted in some distortion of the BChl organization relative to the native one.

After submission of this manuscript, a detailed study of both absorption, as well as fluorescence dichroism on single chlorosome level has been published.[45] That study reported wide distributions of both the single chlorosome modulation depths in absorption as well as fluorescence. Furthermore, the individual chlorosomes showed a wide distribution in the positions as well as the widths of their emission bands. Since these optical properties are determined by the exciton structure of the BChl aggregates, which in turn is determined by the details of the BChl arrangement, the conclusion of that study was that chlorosomes of the w.t. *C. tepidum* showed large structural disorder reflecting both ensemble disorder, as well as mesoscopic inner structural disorder because of large variations in the BChl arrangements in one single chlorosome. We note that the experimental conditions for that study were quite similar to ours, that is, chlorosomes were attached to the surface of a glass plate. Our data are clearly at variance with the properties of the chlorosome preparation studied in that work even at the level of the most basic optical properties. For example, our preparation does not show any significant ensemble heterogeneity, that is, the chlorosomes in our study have all the same peak positions and widths of their fluorescence within the error limits and excellent agreement with the bulk properties. Likewise the polarization properties of single chlorosomes in our preparation of w.t. chlorosomes do not show a wide distribution. We thus conclude that the wide distributions in all the optical properties found in the study of Furumaki et al. do originate from bulk and/or mesoscopic disorder introduced either by the growth conditions of the bacteria or by the applied isolation/handling procedure. The very narrow distributions of these optical properties in our data indicate the lack of significant disorder and imply that undisturbed native chlorosomes do indeed have very regular internal BChl aggregate structures.

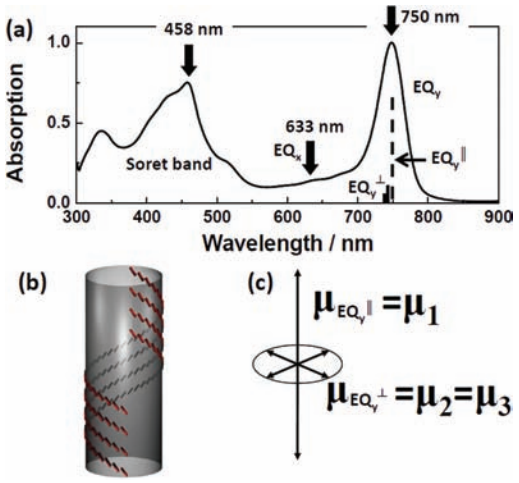


**Figure 8.** (a) Absorption spectrum of chlorosomes in solution. Exciton bands (including their polarization) according to the LD experimental result[30] corresponding to different peaks in the spectrum are indicated schematically. The thick arrows indicate the excitation wavelengths used in this study. (b) The cylindrical structure[22] and (c) the dipole moment components for the tubular aggregates, See Scheme1 for the definition of the parameters.

**Excitonic Transitions and Internal Organization of BChls.** The optical properties of chlorosomes are dominated by the strong excitonic coupling of the BChls arranged as J-type aggregates, which results in, for example, the red shift of the spectra in comparison to free BChls.[46−48] The electronic transitions of the monomeric BChl c, which is actually a chlorophyll-a molecule in terms of the $\pi$-electronic structure, are well-known.[49,50] The lowest transition dipole of BChl c (corresponding to $Q_y$ band in absorption) is reported to deviate slightly from the molecule plane and almost perpendicular to the higher energy transition dipole moment ($Q_x$ band in absorption).[51] The Soret band situated at 400−500 nm is a mixture of different transitions. In the chlorosomes, different exciton transitions originate from different transitions of the interacting BChls.[52] The excitonic $Q_y$ band (we will call it $EQ_y$ hereafter) still has the lowest energy located at ∼750 nm. The excitonic Soret band can still be understood as a combination of $EB_y$ and $EB_x$ transitions, which are oriented almost perpendicularly to each other. The $EB_y$ band has a lower energy than the $EB_x$ band and is located at ∼460 nm based on the 3D LD spectral data.[30,52] The fluorescence of chlorosomes originates, independently of the excitation wavelength, from the $EQ_y$ transition (lowest energy state). Thus the modulation depth in fluorescence should only depend on the $EQ_y$ exciton transition dipole moments, and it must reflect the organization of BChls inside the chlorosome.

Cylindrical organization BChls has been used the most to account for the properties of the exciton transitions, and as it will be shown below, it predicts the polarization properties of individual chlorosomes in excellent agreement with our experiments.

Calculations of exciton band structure and polarization of exciton transition in cylindrical systems have been done for tubular J-aggregates[53−57] and also applied to chlorosomes.[47,48,52] Exciton theory shows that the optically accessible exciton states close to the bottom of the band (the states forming $EQ_y$ band) can be split into two groups. Transition dipole moments of the states from the first group are parallel to the cylinder axis, while in the second group are perpendicular to the axis[11,48,53,57] (Figure 8). Note this is the case even for an ideal cylindrical aggregate without any disorder.

For the particular BChls arrangements used in the cited publications for exciton band calculations (Figure 8b)) the energy separation between the strongest perpendicularly polarized transitions is smaller than the thermal energy kT at room temperature[48] and even smaller than the observed absorption line width. Therefore, for a real chlorosome because of the energetic disorder (inhomogeneity of the exciton band in within an individual chlorosome) all exciton transitions regardless of their polarization contribute to the absorption band $EQ_y$ (maximum at 750 nm). Fluorescence is also coming from the states of the both orientations of the transition dipole moment due to thermal population of the corresponding exciton states. In agreement with our experiment, the theory predicts the cylindrical symmetry of the total exciton transition dipole moment in individual cylinders (chlorosomes) and polarization modulation depth less than unity. The ratio of the total transition dipole moments of these two groups ($\mu_1/\mu_2$) defines the modulation depth. It depends on the exciton delocalization length (coherent length) and the orientation of the transition dipole moments of the monomer molecules and the diameter of the cylinders. The experimentally obtained modulation depth of 0.77 corresponds to $\mu_1/\mu_2 = 1/0.36$ which fits to the theoretical calculations based on an ideal concentric tubular organization of BChls[48] taking into account the known large delocalization length of the excitons in chlorosomes.

In the undulated lamellar model, the chlorophylls are organized in wavy sheets, which are parallel to each other (Figure 1b). Because of the asymmetry of the structure the polarization properties should be different when measuring from different sides. Therefore, only at highly restrictive conditions (Scheme 1 blocks 3 and 6), this model can be consistent with our experiment. Theoretically, there is an undulated lamella structure, which may possess cylindrical symmetry of the dipole moment. This is a highly ordered lamellar structure consisting of consecutive half-cylinders. The necessary condition would be that the exciton length is substantially smaller than the half-cylinder circumference so the exciton does not "feel" that the cylinder is not full. However, this situation has been excluded based on the EM data.[22,48]

**Excitation Wavelength Dependence of the Modulation Depth ($M_a$).** The absorption modulation depth was found to depend on the excitation wavelength while the phase shift did not. For all excitation wavelengths the phase shift distributions are centered around zero (Figure 6) with a standard deviation given by the accuracy of the experimental technique. This means that the phases of absorption and fluorescence are always the same, even though the modulation depths are different. According to the reported assignments of the exciton bands[30] (Figure 8a), the 458, 633, and 750 nm excitations are expected to excite the $EB_y$, $EQ_x$, and $EQ_y$ exciton transitions, respectively. For 750-nm-excitation, the absorption and fluorescence originate from the same set of exciton transitions ($EQ_y$ band). In agreement with this the experimental absorption and fluorescence modulation depths were the same with the phase shift equal to zero. However, for 458-nm-excitation, due to the mixing between different transitions occurring in the Soret region the $EB_x$ transition, which is perpendicularly orientated to $EB_y$, was probably also partially excited. We thus expect a reduced absorption modulation depth without any change in the phase shift, in agreement with the experimental results. When excited at 633 nm, where the $EQ_x$ is expected to be located, the modulation depth was quite low (0.38). This can be explained by assuming that a mixture of the $EQ_y$ and $EQ_x$ transitions was excited. The mixing of two perpendicular transitions reduces the modulation depth. For modulation depth equal to 0.38, the ratio between the main axis and the short axis dipole moment components should be about 3:2. This means that the oscillator strength of $EQ_x$ is lower for 633 nm[48] excitation and the tail of the $EQ_y$ band (polarized along the main axis) gives a ∼2.3 times higher absorption than the $EQ_x$ band itself and thus acts as the main component resulting in zero phase shift. Thus, these results are in good agreement with the reported LD data.[30]

**Effect of the Light Conditions.** The experiments reported in the current contribution were also carried out with chlorosome from w.t. *C. tepidum* bacteria grown under very low light condition. It is concluded that the light intensity during the cell growth do not have any substantial effect on the fluorescence spectra or polarization properties of the individual chlorosomes (Figure S5, S6, and S7 in Supporting Information). This indicates that the ratio of the three components $\mu_1/\mu_2/\mu_3$ of the total excitonic dipole moment does not depend significantly on the light conditions during growth and thus, most likely, the internal structure of the chlorosomes is robust, even though the total size of the chlorosomes and also the carotenoid content do change.

## CONCLUSION

Polarizations in absorption and fluorescence were obtained at the same time for individual chlorosomes. Different excitation wavelengths (458, 633, and 750 nm) were used to selectively excite different transitions. For the first time, narrowly distributed modulation depths were observed for all the wavelengths indicating that all the chlorosomes are essentially identical in terms of their polarization properties. The data allowed us to prove cylindrical symmetry of the total transition dipole moment of individual chlorosomes. Such symmetry is inherent to the cylindrical structure of the chlorosome internal organization.

## ASSOCIATED CONTENT

**Supporting Information.** Concentration dependence, detailed description of the 2D polarization SMS, phase shift histogram of WTHL chlorosomes with different excitation wavelength, and 2D results for WTLL chlorosomes. These materials are available free of charge via the Internet at http://pubs.acs.org.

## AUTHOR INFORMATION

**Corresponding Author**

Ivan.Scheblykin@chemphys.lu.se (I.G.S.); holzwarth@mpi-muelheim.mpg.de (A.R.H.)

[#]A preliminary account of this work has been presented at the *Light Harvesting Satellite Meeting of the 15th International Congress on Photosynthesis*, Tianjin, China, August, 2010.

## ■ ACKNOWLEDGMENT

This study was financially supported by The Swedish Research Council, The Royal Physiographic Society in Lund, the Knut & Alice Wallenberg Foundation, the Crafoord Foundation, and the Carl Trygger Foundation. Y.T. thanks the Swedish Institute for a postdoctoral scholarship. I.G.S. is grateful for a Linnaeus Grant to Lund Laser Centre.

## ■ REFERENCES

(1) Olson, J. M. In *Encyclopedia of Biological Chemistry*; Lennarz, W. J., Lane, M. D., Eds.; Elsevier: New York, 2004; pp 325−330.
(2) Röger, C.; Müller, M. G.; Lysetska, M.; Miloslavina, Y.; Holzwarth, A. R.; Würthner, F. *J. Am. Chem. Soc.* **2006**, *128*, 6542–6543.
(3) Röger, C.; Miloslavina, Y.; Brunner, D.; Holzwarth, A. R.; Würthner, F. *J. Am. Chem. Soc.* **2008**, *130*, 5929–5939.
(4) Ganapathy, S.; Sengupta, S.; Wawrzyniak, P. K.; Huber, V.; Buda, F.; Baumeister, U.; Würthner, F.; de Groot, H. J. M. *Proc. Natl. Acad. Sci. U. S. A.* **2009**, *106*, 11472–11477.
(5) Holzwarth, A. R.; Griebenow, K.; Schaffner, K. *Z. Naturforsch. C* **1990**, *45*, 203–206.
(6) Holzwarth, A. R.; Griebenow, K.; Schaffner, K. *J. Photochem. Photobiol., A* **1992**, *65*, 61–71.
(7) Balaban, T. S.; Tamiaki, H.; Holzwarth, A. R. In *Supramolecular Dye Chemistry*; Wurthner, F., Ed.; Springer-Verlag: Berlin, 2005; pp 1−38.
(8) Oostergetel, G. T.; van Amerongen, H.; Boekema, E. J. *Photosynth. Res.* **2010**, *104*, 245–255.
(9) Scheblykin, I. G.; Sliusarenko, O. Y.; Lepnev, L. S.; Vitukhnovsky, A. G.; Van der Auweraer, M. *J. Phys. Chem. B* **2000**, *104*, 10949–10951.
(10) Scheblykin, I. G.; Varnavsky, O. P.; Bataiev, M. M.; Sliusarenko, O.; Van der Auweraer, M.; Vitukhnovsky, A. G. *Chem. Phys. Lett.* **1998**, *298*, 341–350.
(11) Prokhorenko, V. I.; Holzwarth, A. R.; Müller, M. G.; Schaffner, K.; Miyatake, T.; Tamiaki, H. *J. Phys. Chem. B* **2002**, *106*, 5761–5768.
(12) Brune, D. C.; Nozawa, T.; Blankenship, R. E. *Biochemistry* **1987**, *26*, 8644–8652.
(13) Feiler, U.; Albouy, D.; Lutz, M.; Robert, B. *Photosynth. Res.* **1994**, *41*, 175–180.
(14) Hildebrandt, P.; Tamiaki, H.; Holzwarth, A. R.; Schaffner, K. *J. Phys. Chem.* **1994**, *98*, 2192–2197.
(15) Hildebrandt, P.; Griebenow, K.; Holzwarth, A. R.; Schaffner, K. *Z. Naturforsch. C* **1991**, *46*, 228–232.
(16) Nozawa, T.; Suzuki, M.; Ohtomo, K.; Morishita, Y.; Konami, H.; Madigan, M. T. *Chem. Lett.* **1991**, 1641–1644.
(17) van Amerongen, H.; van Haeringen, B.; van Gurp, M.; van Grondelle, R. *Biophys. J.* **1991**, *59*, 992–1001.
(18) Kunieda, M.; Tamiaki, H. *J. Org. Chem.* **2009**, *74*, 5803–5809.
(19) Holzwarth, A. R.; Schaffner, K. *Photosynth. Res.* **1994**, *41*, 225–233.
(20) Balaban, T. S.; Holzwarth, A. R.; Schaffner, K.; Boender, G. J.; de Groot, H. J. M. *Biochemistry* **1995**, *34*, 15259–15266.
(21) Egawa, A.; Fujiwara, T.; Mizoguchi, T.; Kakitani, Y.; Koyama, Y.; Akutsu, H. *Proc. Natl. Acad. Sci. U. S. A.* **2007**, *104*, 790–795.
(22) Ganapathy, S.; Oostergetel, G. T.; Wawrzyniak, P. K.; Reus, M.; Chew, A. G. M.; Buda, F.; Boekema, E. J.; Bryant, D. A.; Holzwarth, A. R.; de Groot, H. J. M. *Proc. Natl. Acad. Sci. U. S. A.* **2009**, *106*, 8525–8530.
(23) Pšenčik, J.; Ikonen, T. P.; Laurinmäki, P.; Merckel, M. C.; Butcher, S. J.; Serimaa, R. E.; Tuma, R. *Biophys. J.* **2004**, *87*, 1165–1172.
(24) Pšenčik, J.; Arellano, J. B.; Ikonen, T. P.; Borrego, C. M.; Laurinmäki, P. A.; Butcher, S. J.; Serimaa, R. E.; Tuma, R. *Biophys. J.* **2006**, *91*, 1433–1440.
(25) Pšenčik, J.; Collins, A. M.; Liljeroos, L.; Torkkeli, M.; Laurinmäki, P.; Ansink, H. M.; Ikonen, T. P.; Serimaa, R. E.; Blankenship, R. E.; Tuma, R.; Butcher, S. J. *J. Bacteriol.* **2009**, *191*, 6701–6708.
(26) Saga, Y.; Tamiaki, H. *J. Biosci. Bioeng.* **2006**, *102*, 118–123.
(27) Oostergetel, G. T.; Reus, M.; Chew, A. G. M.; Bryant, D. A.; Boekema, E. J.; Holzwarth, A. R. *FEBS Lett.* **2007**, *581*, 5435–5439.
(28) Blankenship, R. E.; Olson, J. M.; Miller, M. In *Anoxygenic Photosynthetic Bacteria*; Blankenship, R. E., Madigan, M. T., Bauer, C. E., Eds.; Kluwer: Dordrecht, the Netherlands, 1995; pp 399−435.
(29) Ma, Y. Z.; Cox, R. P.; Gillbro, T.; Miller, M. *Photosynth. Res.* **1996**, *47*, 157–165.
(30) Tamiaki, H.; Tateishi, S.; Nakabayashi, S.; Shibata, Y.; Itoh, S. *Chem. Phys. Lett.* **2010**, *484*, 333–337.
(31) Griebenow, K.; Holzwarth, A. R.; van Mourik, F.; van Grondelle, R. *Biochim. Biophys. Acta* **1991**, *1058*, 194–202.
(32) Furumaki, S.; Habuchi, S.; Vacha, M. *Chem. Phys. Lett.* **2010**, *487*, 312–314.
(33) Shibata, Y.; Saga, Y.; Tamiaki, H.; Itoh, S. *Photosynth. Res.* **2009**, *100*, 67–78.
(34) Shibata, Y.; Saga, Y.; Tamiaki, H.; Itoh, S. *Biochemistry* **2007**, *46*, 7062–7068.
(35) Mirzov, O.; Bloem, R.; Hania, P. R.; Thomsson, D.; Lin, H. Z.; Scheblykin, I. G. *Small* **2009**, *5*, 1877–1888.
(36) Wahlund, T. M.; Woese, C. R.; Castenholz, R. W.; Madigan, M. T. *Arch. Microbiol.* **1991**, *156*, 81–90.
(37) Gerola, P. D.; Olson, J. M. *Biochim. Biophys. Acta* **1986**, *848*, 69–76.
(38) Lin, H. Z.; Tabaei, S. R.; Thomsson, D.; Mirzov, O.; Larsson, P. O.; Scheblykin, I. G. *J. Am. Chem. Soc.* **2008**, *130*, 7042–7051.
(39) van Walree, C. A.; Sakuragi, Y.; Steensgaard, D. B.; Bösinger, C. S.; Frigaard, N. U.; Cox, R. P.; Holzwarth, A. R.; Miller, M. *Photochem. Photobiol.* **1999**, *69*, 322–328.
(40) Wang, J.; Brune, D. C.; Blankenship, R. E. *Biochim. Biophys. Acta* **1990**, *1015*, 457–463.
(41) Shibata, Y.; Saga, Y.; Tamiaki, H.; Itoh, S. *Biophys. J.* **2006**, *91*, 3787–3796.
(42) Saga, Y.; Wazawa, T.; Mizoguchi, T.; Ishii, Y.; Yanagida, T.; Tamiaki, H. *Photochem. Photobiol.* **2002**, *75*, 433–436.
(43) Betti, J. A.; Blankenship, R. E.; Natarajan, L. V.; Dickinson, L. C.; Fuller, R. C. *Biochim. Biophys. Acta* **1982**, *680*, 194–201.
(44) Saga, Y.; Shibata, Y.; Tamiaki, H. *J. Photochem. Photobiol., C* **2010**, *11*, 15–24.
(45) Furumaki, S.; Vacha, F.; Habuchi, S.; Tsukatani, Y.; Bryant, A. D.; Vacha, M. *J. Am. Chem. Soc.* **2011**, *133*, 6703–6710.
(46) Linnanto, J. M.; Korppi-Tommola, J. E. I. *Photosynth. Res.* **2008**, *96*, 227–245.
(47) Prokhorenko, V. I.; Steensgaard, D. B.; Holzwarth, A. R. *Biophys. J.* **2000**, *79*, 2105–2120.
(48) Prokhorenko, V. I.; Steensgaard, D. B.; Holzwarth, A. R. *Biophys. J.* **2003**, *85*, 3173–3186.
(49) Hoff, A.; Amesz, J. In *Chlorophylls*, Scheer, H., Ed.; CRC Press: Boca Raton, FL, 1991; pp 723−738.
(50) Scheer, H. In *Chlorophylls*; Scheer, H., Ed.; CRC Press: Boca Raton, FL, 1991; pp 3−30.
(51) Linke, M.; Lauer, A.; von Haimberger, T.; Zacarias, A.; Heyne, K. *J. Am. Chem. Soc.* **2008**, *130*, 14904–14905.
(52) Shibata, Y.; Tateishi, S.; Nakabayashi, S.; Itoh, S.; Tamiaki, H. *Biochemistry* **2010**, *49*, 7504–7515.
(53) Bednarz, M.; Knoester, J. *J. Phys. Chem. B* **2001**, *105*, 12913–12923.
(54) Didraga, C.; Pugžlys, A.; Hania, P. R.; von Berlepsch, H.; Duppen, K.; Knoester, J. *J. Phys. Chem. B* **2004**, *108*, 14976–14985.
(55) Didraga, C.; Knoester, J. *J. Lumin.* **2004**, *110*, 239–245.
(56) Didraga, C.; Knoester, J. *J. Chem. Phys.* **2004**, *121*, 10687–10698.
(57) Lampoura, S. S.; Spitz, C.; Dähne, S.; Knoester, J.; Duppen, K. *J. Phys. Chem. B* **2002**, *106*, 3103–3111.